Decarbonization Analysis for Thermal Generation and Regionally Integrated Large-scale Renewables based on Minutely Optimal Dispatch with a Kentucky Case Study

Donovin D. Lewis[1], Aron Patrick[2], Evan S. Jones[1], Rosemary E. Alden[1], Abdullah Al Hadi[1], Malcolm McCulloch[3], and Dan M. Ionel[1]

[1]SPARK Laboratory, Department of Electrical and Computer Engineering, University of Kentucky, Lexington, KY, USA
[2]PPL Corporation, Allentown, PA 18101, USA and LG&E and KU Energy, Louisville, KY 40202, USA
[3]Department of Engineering Science, University of Oxford, Parks Road, Oxford OX1 3PJ, United Kingdom

Decarbonization of existing electricity generation portfolios with large-scale renewable resources such as wind and solar photovoltaic (PV) facilities is important for a transition to a sustainable energy future. This paper proposes an ultra-fast optimization method for economic dispatch of firm thermal generation using high granularity, one minute resolution load, wind, and solar PV data to more accurately capture the effects of variable renewable energy (VRE). Load-generation imbalance and operational cost are minimized in a multi-objective clustered economic dispatch problem with various generation portfolios, realistic generator flexibility, and increasing levels of VRE integration. The economic feasibility of thermal dispatch scenarios is evaluated through a proposed method of levelized cost of energy (LCOE) for clustered generation portfolios. Effective renewable economics is applied to assess resource adequacy, annual carbon emissions, renewable capacity factor, over generation, and cost to build between thermal dispatch scenarios with incremental increases in VRE penetration. Solar PV and wind generation temporally complement one another in the region studied, and the combination of the two is beneficial to renewable energy integration. Furthermore, replacing older coal units with cleaner and agile natural gas units increases renewable hosting capacity and provides further pathways to decarbonization. Minute-based chronological simulations enable the assessment of renewable effectiveness related to weather-related variability and of complementary technologies, including energy storage for which a sizing procedure is proposed. The generally applicable methods are regionally exemplified for Kentucky, USA including 8 scenarios with 4 major year-long simulated case studies and 176 subcases using high performance computing (HPC) systems.

***Index Terms*—renewable energy, solar PV, wind energy, thermal generation, generation portfolio, decarbonization, optimal economic dispatch, electric power system adequacy.**

I. Introduction

Changes in policy and increased awareness of environmental impacts are driving the development and implementation of technology to significantly reduce greenhouse gas (GHG) emissions including carbon dioxide (CO2). According to the International Energy Agency (IEA), electric power generation around the world accounts for about 40% of energy-related CO2 emissions and offers significant opportunities for emissions reduction with increased variable renewable energy (VRE) generation [1].

One of the major challenges with the integration of increased clean energy is resource adequacy, or the ability to produce sufficient generation to meet customer loads at all hours due to the weather-dependent variability of solar PV and wind resources. Increased renewable penetration requires cost-effective support of firm, agile generation that can turn on quickly when needed and operate as long as needed, and/or long-term energy storage to handle extreme weather, peaking periods, and periods of low renewable generation [2]. Hourly analysis of generation including VRE may not be able to accurately evaluate the capability of firm generation to match demand with rapidly changing VRE power output, which changes realistically at the minutely-scale.

To evaluate pathways for decarbonization through gradually increased renewable penetration backed by firm generation, a method of ultra fast minute to minute (M-M) multi-objective optimization (MOO) was developed for clustered generation economic dispatch and implemented on high performance computing (HPC) systems, as described in the current paper. The proposed general method was applied for a case study in Kentucky, USA using actual load, renewable, and fossil generating unit data provided by the state's largest utility Louisville Gas and Electric and Kentucky Utilities (LG&E and KU), part of the PPL Corporation family of companies. Carbon dioxide emissions from electricity generation in Kentucky have already declined by more than 40% from 2010 through 2021, due primarily to the closure of coal-fired generators and the addition of cleaner-burning natural gas combined cycle and renewables [3], [4]. In the absence of federal or state policy requiring decarbonization, electric utilities operating in Kentucky have voluntarily committed to increase renewable generation and reduce carbon dioxide emissions, with some pledging to achieve net-zero emissions by 2050 [5]. As additional retirements of coal-fired electricity generating units are scheduled to occur before 2035, the important decision arises of what type of generating resources to build next [6].

Minute-to-minute analysis also enables detailed studies into energy storage requirements and imbalance compensation to quantify the mismatch between weather-based generation and expected demand on short and long-term timescales. Economic and CO2 emissions analysis of optimization results were

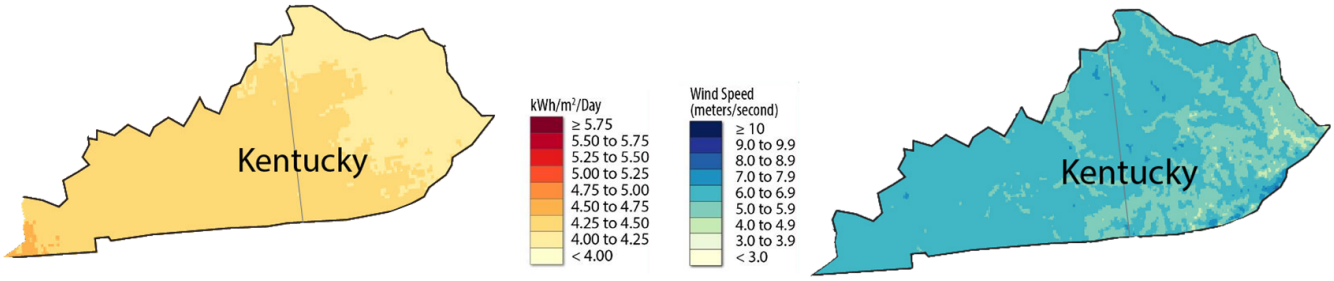

Fig. 1: Maps of Kentucky annual average global horizontal irradiance and wind speed at 100 meter hub height from NREL [7]. Kentucky experiences a mild climate with large seasonal variation, and is located at approximately 37.5°N by -85.29°E.

performed with capital expenditures (CAPEX), cost to build, per clustered generation type, carbon dioxide emissions per generation type, and a proposed method of levelized cost of energy (LCOE) for generation portfolios considering fuel cost and cost of operation.

A first main novel contribution of the research described in the current paper is the ultra-fast optimization of dispatchable generation to minimize generation/demand imbalance and cost for a chronological year of minutely data using high performance computing (HPC) systems. To the authors' knowledge, this study is the first to consider such high resolution in economic dispatch of thermal generation considering operational limitations. A second main contribution is represented by the proposed method for improved energy storage sizing to reduce undergeneration imbalances based on the minutely simulation.

Additional contributions include proposed methods for evaluating the economic and technical feasibility of increased renewable penetration with high seasonal generation variability. A method is proposed for calculating the LCOE of a generation portfolio derived from equations and projections published by the National Renewable Energy Laboratory (NREL) [8]. Minute to minute chronological firm dispatch is used to assess the limitations imposed by operational flexibility and the requirements of energy storage for decarbonization beyond 80%.

The paper is structured as follows: a review of relevant global and regional developments and an introduction to the Kentucky specific studies in the next section, detailed economic load dispatch problem formulation and optimization in Section 3, and minutely simulation cases for various generation mixes with results in Section 4. The results are further analysed in Section 5, including a discussion of the findings with implications to future infrastructure development for renewable generation facilities, zero to low carbon firm generation, and energy storage, based on widely used cost and emission indexes. Concluding remarks are presented in the final section.

II. Global and Regional Developments and Studies

The cost of solar PV and wind power generation has reduced significantly over the last decade; however, the intermittency of these resources limits the maximum amount that can be integrated into the existing generation and transmission system without affecting the reliability of service. For example, during a very sunny day, solar PV units can produce near rated capacity but experience large variability in output early and late in the day, requiring sufficient firm generation ramping capability to maximize energy utilization and effectiveness [9], [10]. On the other hand, a very cloudy day can cause periods of low renewable generation, necessitating enough firm generation capacity to fill the deficit between generation and demand [11].

The current North American Electricity Reliability Corporation (NERC) standard commonly adopted by utilities specifies that the frequency of under-generation events, a loss of load expectation (LOLE), is at most 0.1 days per year or 99.97% reliability [2], [12]. Techno-economic analysis that accounts for firm generation ramping capability to meet expected demand while also minimizing operational cost is necessary to develop feasible pathways of decarbonization. Hence, a growing field in the scientific and technical literature focuses on analyzing the impact of integrating variable renewable energy (VRE) alongside firm generation in future power system planning and operation.

Studies into increased decarbonization, i.e. the reduction of CO2 emissions, exists throughout literature, many of which focus on scenarios for complete generation overhaul including Germany [13], Europe [14], [15], the US [16]–[18], and Southeast Asia [19]. Towards deep decarbonization, i.e. 80 to 100% reduction in CO2 emissions from current levels, more than 40 studies were considered and tabulated in [20] and 88 regional studies summarized in [21]. Within the majority of the papers reviewed, the main focus was placed on deep decarbonization economic feasibility rather than resource adequacy with gradual renewable adoption and none simulated chronologically minute-to-minute. This represents a significant gap in literature that is addressed by the minutely firm generation dispatch method proposed and the case study completed in this paper.

Limitations of short-term weather dependent VRE integration summarized in [22] have found significant mismatch between demand and generation across time scales with increased renewable annual energy contributions. A recent study into VRE integration established feasible regional penetration of solar PV without substantial generation violations through economic dispatch of thermal generation with individual unit commitment [23]. Minute-to-minute unit commitment developed within the study sought to capture the realistic contri-

butions of firm thermal generation to compensate for dips in VRE output due to quick changes in weather.

The impact of realistic unit commitment constraints including built capacity, ramping limits, and turn-down capability significantly affect system reliability simulation and results with increased VRE penetration. Hybrid methods of economic dispatch coupled with thermal generation operational flexibility were published on studies for gradual integration of renewable generation, e.g. [24]–[28].

Hybrid economic dispatch was further developed to group distributed generation units into clusters, combining the constraints on operational flexibility from multiple plants as an energy type [29]. Clustered unit commitment, used in this cited study, has been found to represent unit flexibility with very small difference in optimal solution and is significantly more computationally efficient, up to 15 times faster than individual units at large scale [29]–[31].

To maximize effective techno-economic integration of renewable generation, variability must be compensated for by firm generation or with technologies that shift load or generated energy [22]. The resolution and range of analysis plays a large role in the planning for and solution of supply and demand mismatch at several time scales (diurnal, daily, seasonal). A previous study by other authors identified that higher resolution decarbonization studies, such as the minutely approach proposed in the current paper, are needed to capture the nuanced interactions between system resources and expected cost of generation [32]. It was found that temporal aggregation or time slices, deployed in many previous studies, may not capture fundamental relationships, understate the value of broad technology portfolios, and do not solve time-based mismatch issues [32], [33]. Sub-hourly scheduling and planning is not only beneficial and essential for long-term planning but reduces expected reserves and generator movement to balance supply and demand [33], [34].

A major barrier for widespread deep decarbonization is represented by the seasonal mismatch or long-term mismatch between generation and demand in the winter, when wind and solar output are reduced [22]. Chronological simulation is necessary to capture the challenges of long-term energy deficit due to seasonal variability [27], [32]. Minute-based chronological analysis, not performed in previous papers, models fast variations not captured in typical long-term simulations and is essential for the rating and planning of broad technologies to ensure system reliability.

As proposed and described in the current paper, in order to solve the hybrid clustered economic dispatch with unit commitment constraints, optimization was employed chronologically minute by minute for generation to meet load. Rather than priority list stacking of generation by least cost or conventional numerical optimization, evolutionary optimization was employed to handle the complex formulation without simplification, allowing for future expansion of objectives, constraints, and scalability [26]. A heuristic multi-objective differential evolution (MODE) type algorithm was chosen to identify the optimal Pareto front with comparable results to NSGA-II alternatives at a faster speed. Integrated decision making was used with multi-objective optimization, similar to that proposed in [35], to select a cost-minimizing solution from minimum imbalance options.

The example region studied, Kentucky, is a land-locked service area with a humid subtropical Koppen climate classification (Cfa), characteristic of large seasonal temperature variation [36]. Average solar irradiance and wind speed distribution is similar across the region with small pockets of higher wind generation, as shown in the annual average maps of Fig. 1. Renewable generation distributed across large regions may smooth resource output variability, enabling, in principle, more constant system generation [16], [22], [34]. Still, our analysis of minute-to-minute solar data found that generation may decrease from 100% to 10% capacity in as little time as two minutes. While current solar penetration in Kentucky pose no risk to grid reliability, if all electricity came directly from solar and wind resources, the availability of electricity would fluctuate greatly with the weather.

In the following, multiple scenarios of firm generation sets were considered with varying levels of solar PV and wind penetration to analyze paths of gradual renewable energy integration. Four cases have been simulated with a mixture of firm thermal generation capacity with 44 subcases of increasing renewable penetration and a ratio of 2:1 for solar PV to wind generation. The weather data is from 2018 and includes correlated minutely measured and geospatially-aggregated solar irradiance and wind speed from 60+ weather stations. Within each subcase, the gap between generation and measured minutely load for 2018 was analyzed following generation MOO to minimize system imbalance and operational cost.

III. Economic Load Dispatch Problem Formulation and Optimization

A. Problem Formulation

On the pathway to increased future integration of VRE resources, planning for the cost-effective dispatch of firm, controllable, thermal generation is essential to meet demand due to renewable energy generation variability. A minute-based economic dispatch is used to capture the capabilities of firm generation to complement solar PV and wind power variation towards gradual renewable integration. Objectives for the optimization are to minimize imbalance between generation and load as well as the price of generation operation including fuel/consumables, operation and maintenance, and fuel heat rate using each firm generation type. Decision variables considered for the system are the scheduled generation output from three firm generation types, $i = 1, 2, 3$, i.e. coal and natural gas of the combined cycle and combustion turbine type, respectively, with units distributed across Kentucky.

Thermal generation clustered unit constraints such as ramping rate, i.e. the ability to alter power output in each minute, and generation capacity limits must be considered to evaluate the time constrained output. In clustered unit commitment, the capacity limits are dependent upon the rated power capacity from all distributed units in that group. The power output of each generator, $P_i(t)$, is bounded by two mathematical inequality sets as described by:

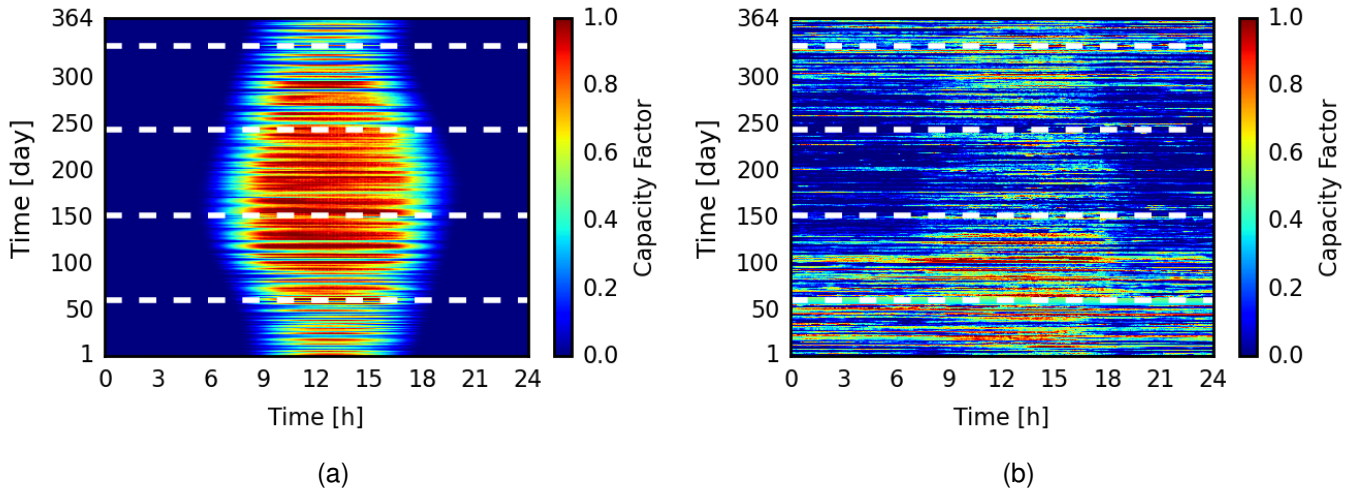

Fig. 2: Kentucky state-wide utility solar PV (a) and land based wind (b) aggregated minutely power generation across the year with white dotted lines differentiating meteorological seasons. Resources were found to be beneficially disjoint and complementary with high output from solar PV in the summer months and wind in the winter months.

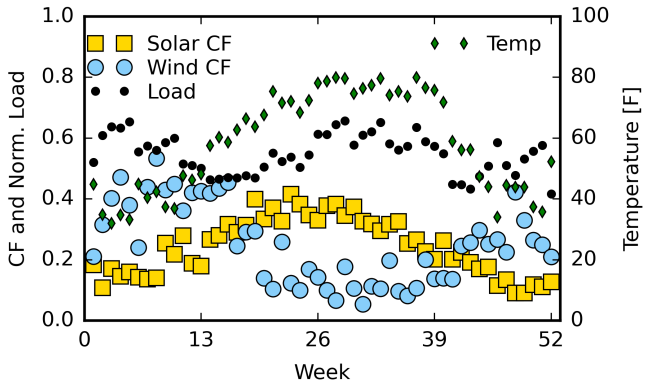

Fig. 3: Average solar PV and wind capacity factor, normalized load, and temperature in Fahrenheit with irradiance for each week across the year. The capacity factors for wind and solar peak in winter and summer, respectively, illustrating the complementary nature of the renewable resources.

$$\begin{aligned} P_{min} \leq P_i(t) \leq P_{max}, \\ P_{max} * -RR_i \leq P_i(t) - P_i(t-1) \leq P_{max} * RR_i, \end{aligned} \tag{1}$$

where a maximum rated capacity, P_{max}, and minimum generation, P_{min} are specified for each generator type, and the power variation for each time step is limited by the generator ramping rate, RR_i.

From these generation-specific operational limits, a power output is selected:

$$\min \Big\{ I(t) = |\sum_{i=1}^{3} P_i(t) + P_{ren}(t) - P_L(t)|, \tag{2}$$

to minimize the power imbalance, $I(t)$, between load, $P_L(t)$, and generation considering renewable, $P_{ren}(t)$, and firm capability, $P_i(t)$.

With a scheduled power output from each generation type, the amount of fuel needed to reach that power output and the overall cost of generation are calculated. Cost per thermal generation dispatch within a minute of scheduling, $P_r(t)$, is calculated by:

$$\min \begin{cases} P_r(t) = |\sum_{i=1}^{3} (C_g + Con_i + MC_i) \cdot P_i(t)|, \\ \text{where } C_g = HR_i \cdot FC_i. \end{cases} \tag{3}$$

where the running cost of the generator, C_g, is a function of the heat rate, HR_i; the fuel cost, FC_i; the fixed cost of consumables for emission reduction, Con_i; and MC_i the fixed cost of system maintenance.

Since thermal generation unit efficiency varies with percentage output for different unit types, heat rate is calculated using the heat requirement for power considering currently scheduled generation following:

$$HR_i = \frac{a \cdot P_i(t)^2 + b \cdot P_i(t) + c}{P_i(t)}, \tag{4}$$

per each generation type with thermal coefficients, a, b, c. Heat rate integration approximates the running cost of thermal generation at selected output power while considering operational limitations.

B. Optimization Method

An augmented multi-objective differential evolution algorithm was developed based on the concept initially proposed in [37] and adapted to find a cost minimizing set of thermal generation that meets minutely demand using a multi-step process of initialization, mutation, crossover, and selection.The optimization was integrated into the hybrid economic dispatch and clustered unit commitment model to select the minimal cost thermal portfolio that minimizes generation / demand imbalance resulting from multiple populations, as depicted in Fig. 4. In the following description of the optimization procedure, population is used in place of iterations or the

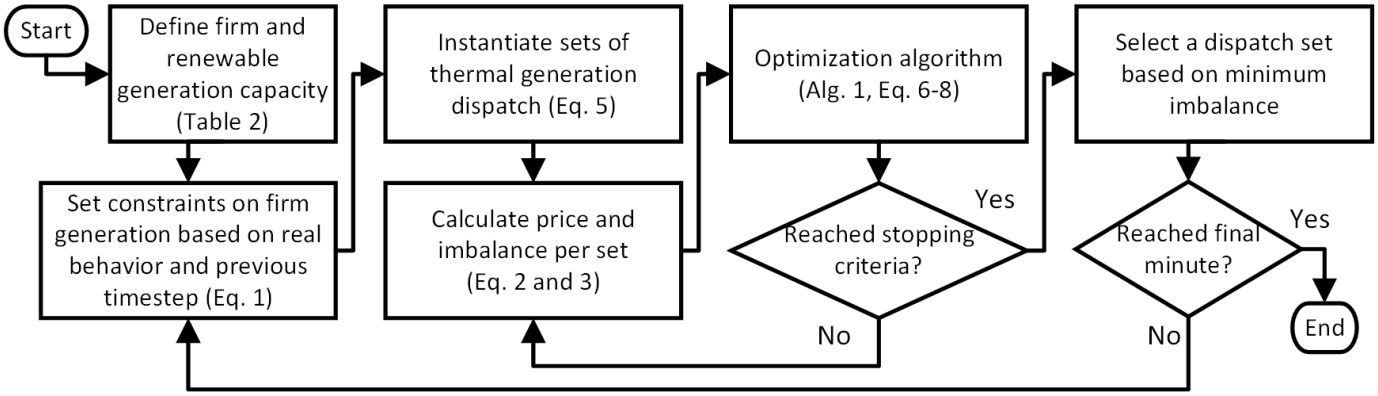

Fig. 4: Proposed procedure for hybrid economic dispatch and clustered unit commitment towards analyzing the limits of renewable generation with operational flexibility. Per scenario, simulations were run chronologically for a year of minutely data to capture high renewable variability.

Algorithm 1 Pseudo-code of the implemented multi-objective optimization algorithm for economic load dispatch based on differential evolution.

Create an initial population $G_{1,p}$ with designs of selected quantities from the firm generation types
while stopping criteria is not satisfied **do**
  for each population, p, in $G_{n,p}$ **do**
    Sample random indices R
    ▷ Mutation
    $G_{M,n,p} \leftarrow G_{n,p}[R[0]] + F(G_{n,p}[R[1]] - G_{n,p}[R[2]])$
    if $RAND(0,1) \leq CR$ **then** ▷ Crossover
      $G_{U,n,p} \leftarrow G_{M,n,p}$
    else
      $G_{U,n,p} \leftarrow G_{n,p}$
    end if
    if $f(G_{U,n,p}) \leq f(G_{n,p})$ **then** ▷ Selection
      $G_{n+1,p} \leftarrow G_{U,n,p}$
    else
      $G_{n+1,p} \leftarrow G_{n,p}$
    end if
  end for
  $n \leftarrow n+1$ ▷ Increment to the next iteration
end while

number of evolution generations in order to avoid possible confusion with electricity generation.

For initialization, the designs (i.e. sets of firm generation output) within an initial population vector of the first generation are determined through uniform randomization:

$$g_{n,p,d} = g_{p,low} + ((g_{p,up} - g_{p,low}) * RAND_p(0,1)), \quad (5)$$

where d is the design index; p, the population index; n, the generation index with $n = 1$ to indicate the first generation; G_{p_low}, the lower population bound; and $G_{p,up}$, the upper population bound.

To expand the search space, the designs within a population $G_{n,p}$ are mutated in order to create a new population ($G_{M,n,p}$):

$$g_{M,n,p,d} = g_{n,p,r1} + F * (g_{n,p,r2} - g_{n,p,r3}), \quad (6)$$

where $r1$, $r2$, and $r3$ are distinct design indices selected from a random permutation that cannot be equal to d, and F is the scaling factor, producing more population diversity as it is increased and is typically set within the range of (0,2) [37]. Based on designs from the target ($G_{n,p}$) and mutated ($G_{M,n,p}$) vectors, the cross-over process determines a vector of trial designs ($G_{U,n,p}$) as follows:

$$G_{U,n,p} = \begin{cases} G_{M,n,p} & \text{if } RAND(0,1) \leq CR \\ G_{n,p} & \text{otherwise,} \end{cases} \quad (7)$$

where CR is the cross-over probability. It should be noted that a random value for each of the individual design variables is generated as denoted by the $RAND(0,1)$ function. The final step of selection compares the evaluations of the objective function for $G_{U,n,p}$ and $G_{n,p}$ to improve the $G_{n,p}$ for the next generation:

$$G_{n+1,p} = \begin{cases} G_{U,n,p} & \text{if } f(G_{U,n,p}) \leq f(G_{n,p}) \\ G_{n,p} & \text{otherwise.} \end{cases} \quad (8)$$

This multi-step process, described in Alg. 1, is repeated until a stopping criteria, represented by the maximum number of iterations, is satisfied. The final population provides a trial vector which populates a Pareto space of optimal designs and represents the trade off between operational cost and total number of imbalances in the system. The minimum imbalance dispatch at the lowest cost is selected per minute due to the potential for large cost penalties for significant, long-lasting imbalances.

For each minutely optimization, the number of populations necessary for the MODE type procedure was trialed from 10 to 400 using the correlated weather and load data across the month of January. For each population size, the amount of short term undergeneration was compared and the reduction trend with the increasing number of populations was noted. To give the best possible results for the case study, optimizations were conducted at the maximum considered of 400 populations per time step. Additions to generation types and operational constraints would require similar checks for the optimization process.

All 176 subcases of solar PV and wind power generation within this study were simulated using Python in parallel

TABLE I: Ramp rates, cost coefficients, and fixed maintenance and operation costs for the three types of thermal generation considered in the case study.

Type	Ramp Rate [%]	a [10^{-3}]	b	c	Fuel Cost [$/MMBtu]	Aux [$/MWh]
NGCC	4	0.000385	7.700745	630.0665	176	1.28
NGCT	20	0.020731	2.741114	753.0348	176	5.65
Coal	1.23	0.000001	10.5	0.00001	196	2.34

TABLE II: Summary of generation portfolio capacity with thermal and renewable energy resources. Solar and wind capacity were varied within sub-cases and simulated to emulate gradual renewable energy integration. All values are in GW.

Case [GW]	Coal	NGCC	NG-CCS	Hydrogen	NGCT	Hydro	Solar	Wind
C	5	.7	0	0	2	.1	.1	0
NG	0	5.6	0	0	2	.1	.1	0
C_S	5	.7	0	0	2	.1	0-20	0
NG_S	0	5.6	0	0	2	.1	0-20	0
C_{SW}	5	.7	0	0	2	.1	0-20	0-10
NG_{SW}	0	5.6	0	0	2	.1	0-20	0-10
CCS_{SW}	0	0	7.6	0	0	.1	0-20	0-10
H_{SW}	0	0	0	7.6	0	.1	0-20	0-10

with each generation portfolio solved on a separate core of a large high-performance computer (HPC). The optimizer used Intel(R) Xeon(R) Gold 6144 CPUs with a frequency of 3.50GHz, which could run 400 iterations per timestep in 1.3 seconds for an overall simulation runtime of approximately 8 days per subcase for 525,600 timesteps. The procedure illustrated in Fig. 4 can be performed for different locations and regions and is scalable to larger power levels.

C. Input Data and Assumptions

Input data for an optimization case study was sourced from measured data across the state of Kentucky and used assumptions for generator operation in-line with actual utilization. Minute resolution load data was measured across the service area of the Louisville Gas and Electric and Kentucky Utilities, part of the PPL Corporation family of companies.

Bounds on operational flexibility are derived from real generator characteristics. Natural gas combustion turbine (NGCT) generation, for example, has regulatory limits on maximum capacity due to it's large emissions output. Coal generation, the slowest to ramp up and with low turn-down flexibility, is used as a base-load with a minimum power output near 40% of rated capacity due to it's long starting/stopping time. Coal maximum capacity varies each day depending on coal generation used to meet load within the year 2021. When the maximum capacity changes between days, so does the minimum base load generation. Natural gas generation comprises two types: combined cycle (NGCC) and combustion turbine. The ramp rate, heat rate coefficients, fuel cost, consumables cost for emissions reduction, and maintenance cost for fuel generation types are summarized in Table I.

Capacity factor of solar PV and wind turbine power output is defined as the ratio of current output to maximum capacity and was derived from measured data and expected device paramters. Solar irradiance and wind characteristics, which were employed to create an aggregated capacity factor, were collected from the MesoNet, a network of 60 weather stations distributed throughout Kentucky [38]. Wind turbine capacity factor was derived from wind speed assuming a cut-in speed of 2.5 m/s, a nameplate wind speed of 13 m/s, and a cut-out wind speed of 30 m/s.

The solar PV capacity factor corresponds to one of the best case generation scenarios with relatively predictable power output through the day and low cloud cover as shown in Fig. 2(a). The wind capacity factor, while suffering from relatively large variability, complements daily solar cycle generation and seasonal power output reduction with generation during the night and across the colder months, as illustrated in Fig. 2(b). As an illustration of the solar and wind resources, average capacity factors per week are plotted in Fig. 3 together with temperature measurements sourced from data collected at the E.W. Brown solar farm owned by LG&E and KU [39]. The combination of temperature and capacity factors indicate a strong potential for synergistic renewable deployment with wind peaking in the colder months and solar peaking in the warmer months.

For each predefined mixture of firm generation types, 44 sub-cases of varying renewable penetration were simulated with a 2:1 ratio of solar power to wind power generation. Factors not included in the modeling were transmission losses, interconnection costs for improvement, stability analysis, and transmission line limitations. Trading or transfer between external regions is not considered and all energy is generated and consumed within the region. The maximization of VRE utilization was prioritized and sufficient land surface (acreage) was assumed to be available for renewable deployment. Additionally, all generation was assumed to be available for commitment across the year with no downtime or maintenance required.

IV. Minutely Economic Dispatch Case Studies

A. Pathways to Decarbonization Scenarios

Eight scenarios were proposed and studied to better understand the impact of thermal generation operational constraints with gradually integrated VRE generation. Four of these scenarios were optimized using economic dispatch while the remaining four were derived for cost and emissions analysis. Within each scenario, firm capacity portfolios were defined such that their combined capacity would meet the current generation capability within the LG&E and KU service area.

The four simulated scenarios are meant to capture the influence of gradual integration of solar and wind resources

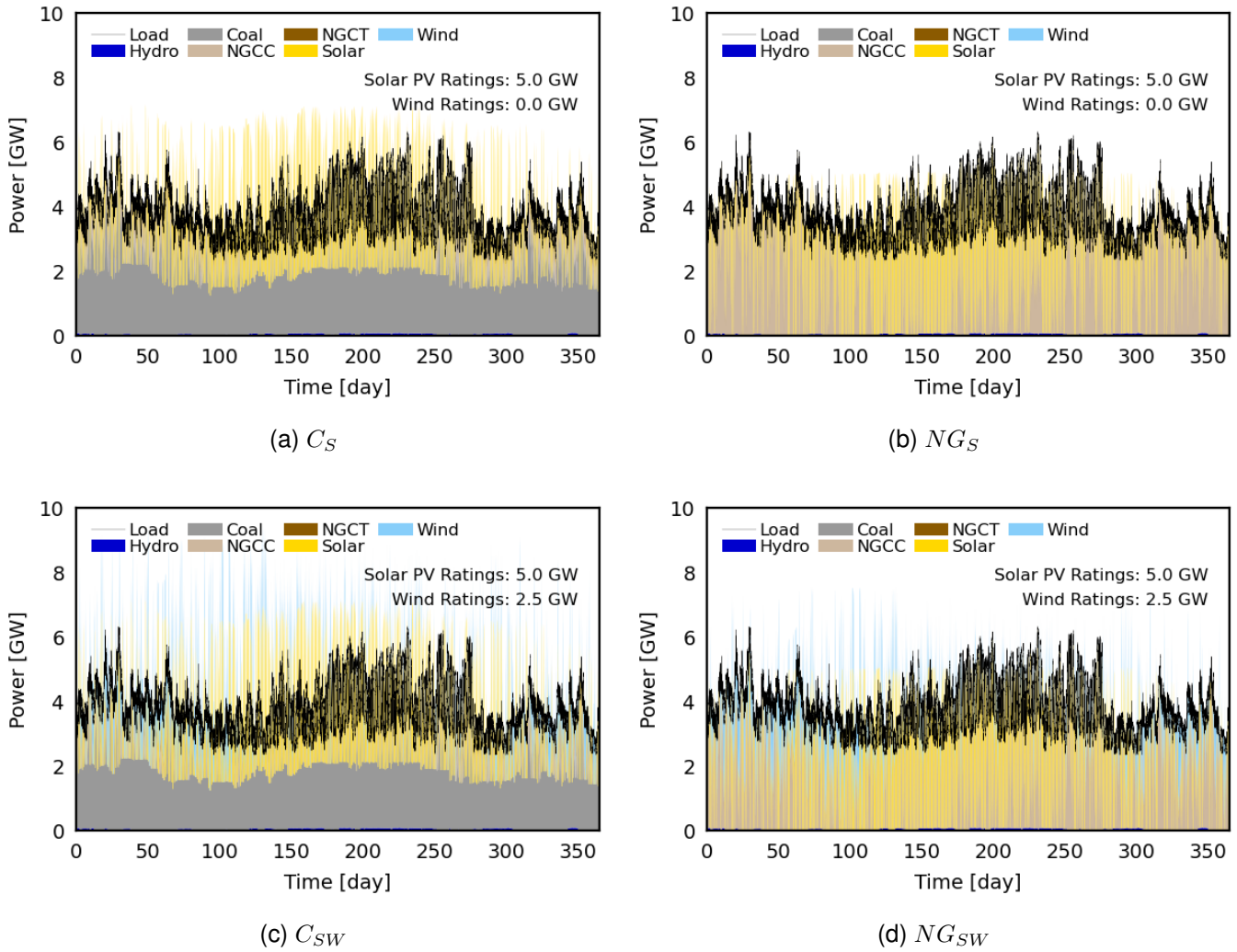

Fig. 5: Full year minutely simulation of optimal power dispatch for 4 decarbonization scenarios. Compared to natural gas at the same solar PV ratings, coal-dominant cases suffer from a significant under-utilization of available VRE generation.

and firm generation flexibility: C_S, the current energy portfolio with solar; C_{SW}, the current portfolio with solar and wind; NG_S, replacing all coal with natural gas and solar; and NG_{SW}, natural gas-dominant generation with solar and wind. The additionally derived scenarios include the current generation portfolio, C; the current portfolio converted to all natural gas, NG; the introduction of carbon capture and sequestration, CCS_{SW}; and the introduction of hydrogen fuel cells, H_{SW}.

Gradual renewable adoption was simulated within each scenario by varying the rated capacity for solar PV from 0 to 20GW and for wind turbines from 0 to 10GW. In order to assess the VRE penetration impacts and effective economics, the maximum capacity of solar PV and wind was sized to supply two times the maximum demand. For the example land-locked region of Kentucky, hydropower is limited in availability to a maximum 143 MW. The generation portfolios studied for each scenario are summarized in Table II.

B. Simulation Results

Economic dispatch results with increasing penetration varied significantly depending on the season and mixture of firm thermal generation. For coal-dominant cases, it was found that renewable integration is limited due to low ramp rates and turn down capability of the coal generation. Natural gas dominant generation benefits from more agile ramp rates and turn down capabilities, allowing larger renewable capacity integration. In the full year results for the four simulated cases shown in Fig. 5 the coal-dominant cases (a) and (c) have to curtail renewable generation significantly as compared to natural-gas dominant cases (b) and (d).

Two weeks are exemplified from case C_{sw} in Figs. 6(a) and 6(b), one with the highest combined average renewable capacity factor from May 8 through 14th and one with the lowest from January 8 to 14th, respectively. It is visualized that when significant overgeneration occurs it can not be used to meet demand due to the inflexiblity of baseload operation from coal. Additionally, the limited flexibility of generation leads to large utilization of NGCT in the low capacity week

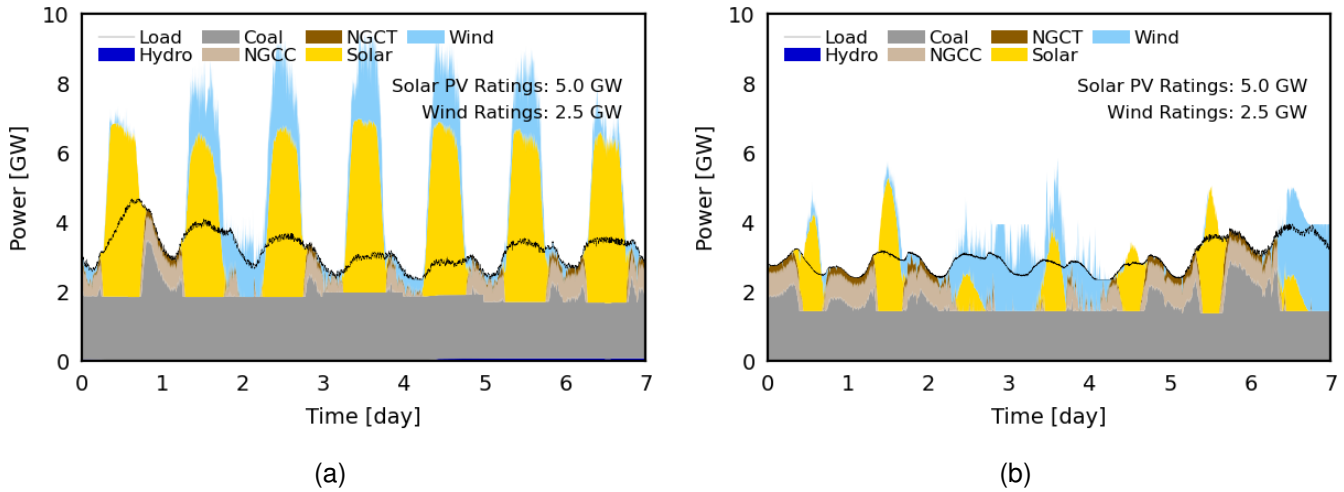

Fig. 6: Example weeks of economic dispatch with a coal-dominated scenario for (a) a high renewable capacity factor week from May 8-14 and (b) low renewable capacity factor week from January 8-14. Renewable output may need to be significantly curtailed compared to natural-gas dominant generation due to slow turn-down and start-up times specific to coal operation as a base load.

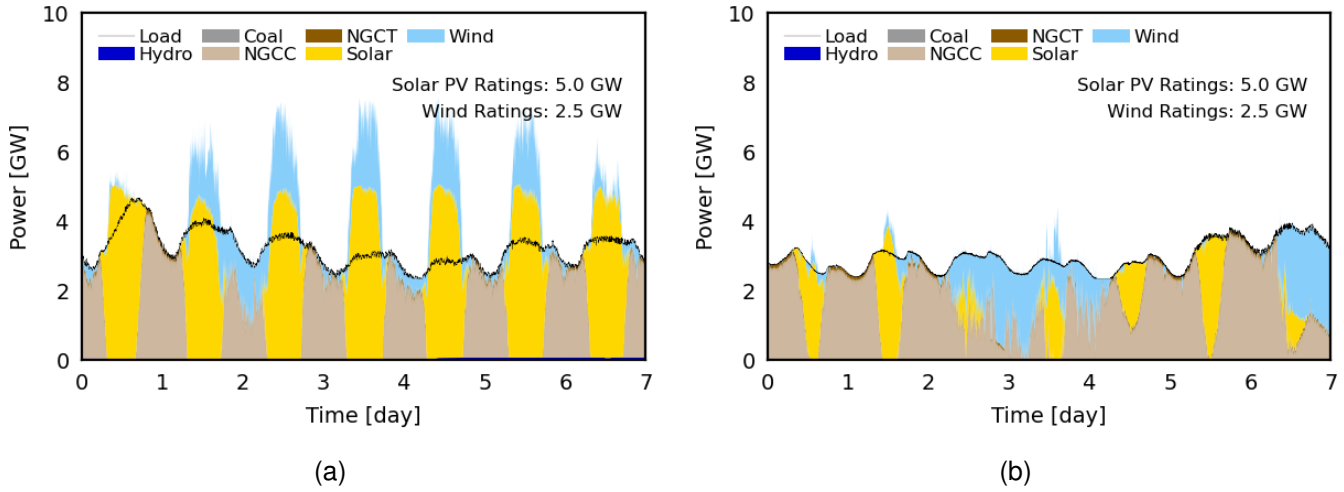

Fig. 7: Example weeks of economic dispatch with a natural gas-dominated scenario for (a) a high renewable capacity factor week from May 8-14 and (b) low renewable capacity factor week from January 8-14. Utilization of natural gas-dominant generation allows for greater renewable potential due to faster ramping rates.

in Fig. 6(b) to close the gap, costing more to operate and in CO2 emissions.

Natural gas-dominated firm dispatch mixtures from the NG_{sw} case are shown in Fig. 7 with significantly increased VRE utilization in 7(a) and sufficient NGCC capacity and ramping capabilities to close gaps without requiring NGCT in Fig. 7(b). The transition from coal to natural gas dominant generation enables greater potential to decarbonize with the gradual integration of VRE resources, while greatly decreasing thermal generation emissions.

Solar and wind resources are expected to complement one another because solar PV generation outputs during the day and wind generation yielding considerable output during the night. Seasonal variation also drastically changes output with maximal solar capacity factor in the summer, while wind capacity factor is improved in the cooler months (see also Fig. 3). The combination of solar and wind resources allows for more renewable penetration than either solar and wind alone due to their time shifted generation periods.

V. Results and Discussion

A. Technical Feasibility

In order to ensure both the technical and the economic feasibility, the resource adequacy for the four scenarios of mixed firm generation with increasing VRE was studied for imbalances represented by the difference between load demand and generation. Limits for minute averaged generation power deficits with an interconnection-dependent tolerance may be defined by regulators [12], [40], or have been proposed in the scientific literature, e.g. [41], [42]. The levels of long-term imbalance considered in the following case study are larger

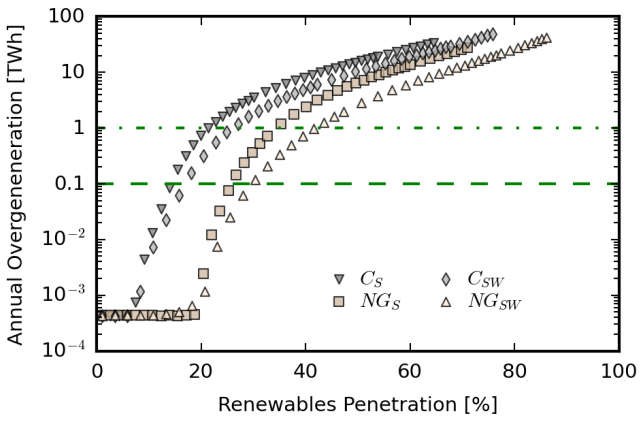

Fig. 8: Annual overgeneration for four generation portfolios plotted together with two example imbalance levels at 0.1 and 1 TWh, respectively.

than .1 GW, or 1.5% of the maximum expected load, and are lasting longer than 15 consecutive minutes.

Under optimal dispatch, none of the four scenarios suffer from long term undergeneration even at high VRE penetration indicating resource adequacy for all four scenarios with the accompanying thermal generation. For the case studies, energy storage or peaking reserves rated at 100MW, 25MWh can handle short-term imbalances with no limitations on the ramping rate. Solar resource output benefits of lower variability resulting from widely spatially distributed generation. The introduction of wind resources may increase short-term undergeneration due to large minute-to-minute variability relative to the thermal generation ramping capability.

Of the four optimized scenarios, there are two major groups, coal-dominant cases with a baseload and small ramping rate, colored in grey, and natural gas-dominant cases with two variant generation types of slower and faster ramping rates, colored in beige. Total annual overgeneration is depicted in Fig. 8 with four distinct trends correlated to the dominant thermal generation type and the combination of solar and wind. Renewable penetration, used throughout for the differentiation between subcases, is defined as the ratio of annual renewable energy generation to annual energy generation throughout the year.

Within all four thermal generation mixtures, a limit level may be considered for integrated VRE capacity related to significant annual overgeneration. At low values of overgeneration, under two example levels of 0.1 and 1 TWh respectively, natural gas-dominant cases can effectively use approximately double the amount of renewables without significant curtailment compared to coal-dominant generation. This effect benefits of the increased operational flexibility of natural gas generation including ramp rate and turn down capabilities. Overall, the integration of both solar PV and wind generation allows for increased effectiveness due to distributed temporal generation and seasonal capacity factor variation with wind being better in the winter and night and solar PV being best during summer days.

B. Effective Renewable Integration

To analyze the impact of VRE introduction on CO2 emissions over time, carbon intensity can be approximated as the product of thermal generation per minute and the median of the published total life cycle emissions factor per generation technology recently published by NREL [43]. Example results for coal and natural gas dominant generation are shown in Fig. 9(a) and (b) respectively with Ren. CF as the normalized output of renewable generation relative to maximum capacity. The expected outcome for a theoretical optimization with carbon intensity as a third objective is reflected in Fig. 9(b) as natural gas is scheduled to match demand with half of the carbon emissions of coal. The switch from coal-dominant generation to natural gas-dominant generation halves the expected annual CO2 emissions as it will be later discussed with respect to Fig. 15.

Quick and large spikes in carbon intensity, shown in Fig. 9, occur to compensate for variability and periods of low VRE output in both scenarios correlating with periods of fast ramping. Distributed solar generation with low minute to minute variability ultimately leads to greatly reduced spikes in the intensity of CO2 emissions when compared to more rapidly varying wind power output. Due to the short nature of the large ramping spikes, short-term energy storage may be used to mitigate significant portions of carbon output to compensate for large variability. The heatmaps from Fig. 10 illustrate that the majority of the overgeneration within the studied cases occurs during the daytime hours revealing a potential for shifting the generated energy in time through demand response or storage.

Overgeneration due to high renewables penetration diminishes the benefits of increased renewable energy, as curtailment, trading, or energy storage may be needed to shift excess generation or demand in time. A renewable capacity factor was calculated considering overgeneration from the output of the economic dispatch to quantify deterioration in renewable economics with curtailment:

$$CF = \frac{E_s + E_w - E_o}{8760 \cdot (C_s + C_w)}, \tag{9}$$

where an E_s and E_w are the annual solar and wind energy generation, respectively, and E_o is the annual energy overgeneration, over the 8,760 hours of the year and P_{ms} and P_{mw} are the maximum solar and wind power capacity, respectively. The results for the four scenarios plotted in Fig. 11 show a decline in renewable generation effectiveness with increased penetration and curtailment. Renewable capacity factor for coal-dominant cases diminishes after 17-20% while potential for natural gas-dominant cases decreases after 30-35% due to their faster turn up and turn down rates.

Increased renewable penetration studies revealed constraints towards maximizing renewable economics. The effect of improved operational flexibility of natural gas over coal is reflected in Fig. 8 as more renewable energy can be effectively hosted and integrated into the system. Once a level is reached in VRE penetration, additional capacity fails to contribute to covering demand and limited contributions to emissions

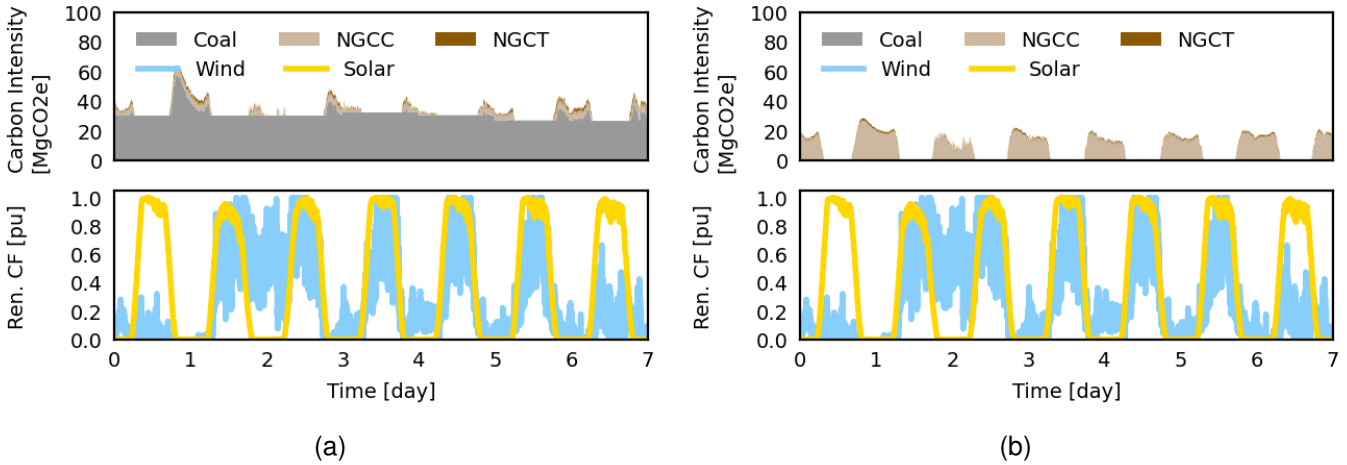

Fig. 9: Example week of economic dispatch carbon intensity for a high renewable capacity factor weeks with (a) coal-dominant support and (b) natural gas-dominant support, respectively. Large spikes in carbon intensity occur in response to renewable power fluctuation. Quick spikes appear to peak and meet demand which can be compensated for with short term energy storage or demand response.

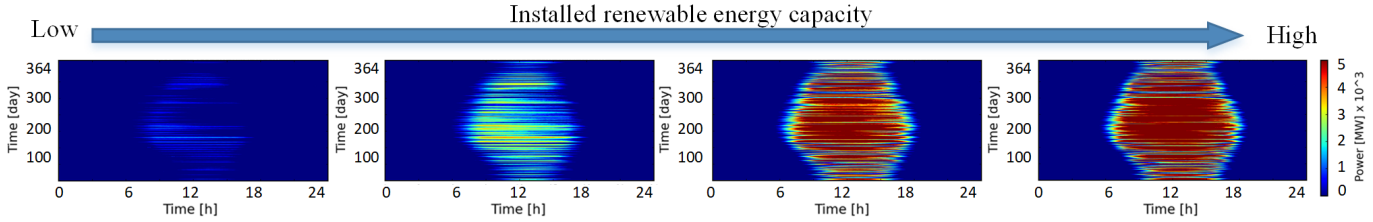

Fig. 10: Positive imbalance magnitude and frequency increase with installed renewable energy capacity as overgeneration does not cover unfulfilled demand. Shifting energy in time to meet temporal mismatch between renewable output and demand increases utilization potential.

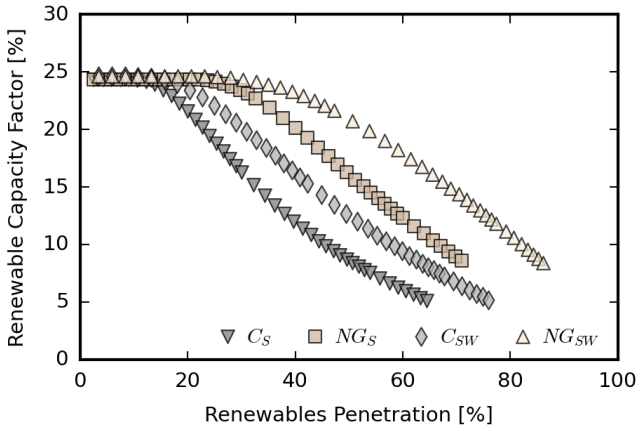

Fig. 11: Capacity factor for the studied cases, including possible curtailment at higher renewable penetration.

reduction may result from VRE output in low capacity periods. Shifting energy demand and/or overgeneration in time and/or the deployment of low-carbon firm generation is beneficial to allow for increased utilization of VRE generation.

C. Uncertainty, Peaking Reserves, and Energy Storage

Previous studies by other authors have discussed the effect on unit commitment of uncertainties, due to, for example, variability in operational downtime, expected load, and renewable energy output [26], [44]. The application of our minute-to-minute proposed method, which is tightly optimized for expected weather data able to capture the inherent variability of wind and solar PV output, would benefit, in principle, of advanced and precise forecasting [34]. Furthermore, in order to assess the capability of peaking reserves and energy storage to compensate for weather-related uncertainty, stochastic evaluation was undertaken. The results of a theoretical comparative weekly example study between the optimal dispatch for a natural gas dominated case to the same dispatch with a 15% largely reduced renewable energy output is presented in Figs. 12(a) and 12(b), respectively.

Minute-based chronological imbalance analysis enables an additional step to systematically size energy storage, such as the battery employed in this theoretical example, to resolve the uncertainty-caused deficit. A proposed post-processing procedure considering energy and power capacities, round trip efficiencies, and self-discharge rates is presented in Fig. 13. The power and energy capacity for the battery was iteratively selected based on undergeneration and overgeneration.

The theoretical example has been purposely selected to illustrate visible differences in Fig. 12 and numerically show how chronological minutely simulation can track relatively small power deficits that can accumulate over time, requiring significantly large energy storage capacity and/or fast-ramping firm generation. The example natural gas dominated case

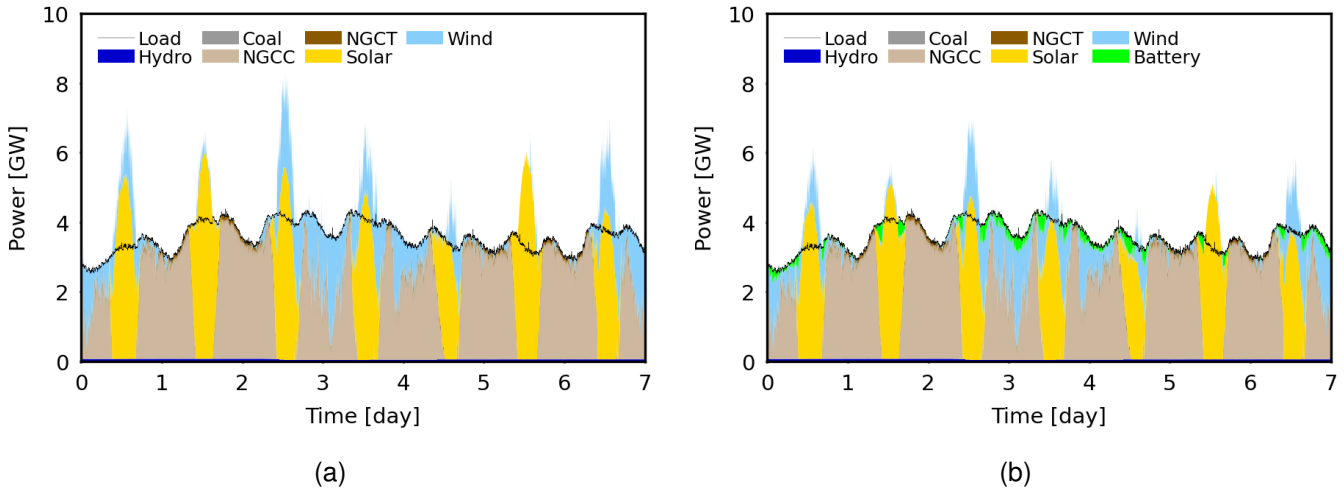

Fig. 12: Example week of economic dispatch for in the critical month of January for a gas dominated system with for 6.5GW solar PV and 3.25GW wind capacity with (a) dispatch with pre-defined weather data and (b) reduction of VRE output by 15% post-dispatch and battery energy storage for matching load demand.

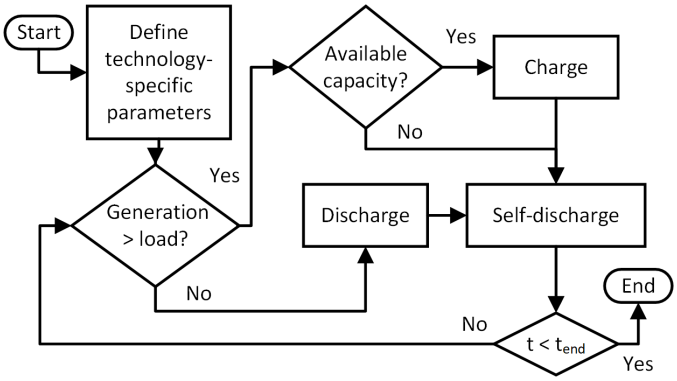

Fig. 13: Proposed procedure for sizing of the energy deficit and potential solutions for a specified generation portfolio. Minute to minute variation largely defines reliability for systems with high renewable energy penetration and can be accounted for using a broad spectrum of technologies to shift energy when needed.

in the critical month of January has 6.5GW solar PV and 3.25GW wind capacity. For a reduction of renewable power output by 15% through the week, energy storage is sized to .5GW and 9GWh to compensate for shortfalls in generation. The very large battery capacity required in this extreme case also highlights the benefit of alternatively employing peaking reserves, such as NGCT generation.

Increased renewable generation integration may expose the power system to sharp changes due to weather variability, necessitating quickly ramping resources and/or energy storage. Time variation of available battery SOC for two case studies of a natural gas dominant scenario is plotted in Fig. 14. The dips in the available SOC correspond to discharging to compensate imbalances on a minute basis. It should be noted that there are only very few and short periods without imbalances, such as those circled in blue in the month of March. There are also sharp drops in renewable power output leading to the very low SOC occurrences circled in green during summer and fall, respectively.

The rising deployment of electric vehicles (EV) opens up additional opportunities for distributed energy storage with managed control for charging and V2G capability [45], [46]. In principle, the EV batteries have great potential for storing renewable overgeneration during the day and for supplying the grid during evening and night. Additionally, mixtures of diverse energy storage systems including hydrogen, and centralized storage may prove greatly beneficial towards meeting the energy deficit due to different operational timescales, efficiencies, and costs [19], [22], [47].

D. Cost to Build per Portfolio

Economic feasibility per scenario was quantified by approximating the cost to build additional generation to the current LG&E and KU generation portfolio, which is specified in Table II as C, using year 2025 capital expenditure (CAPEX) construction costs and approximating the emissions reduction using the annual production per generation type similarly to previously published studies [8], [15], [25]. Table III summarizes the CAPEX construction costs from the 2021 NREL ATB [8]. Per portfolio, the cost to build was estimated as the product of rated generation capacity and that type's CAPEX cost per kW. Emissions rates per generation type were also used as measured from LG&E and KU's generation plants with hydrogen fuel cost to build and emissions approximated based on ongoing research. Renewable energy generation was assumed to be CO2 emission-less.

Eight scenarios were extrapolated from the four optimized cases described prior, assuming the same ramping rate and capacity for different technologies. The resulting CAPEX cost to build and emissions reduction relative to the current Kentucky generation portfolio, C or the large dot, is plotted in Fig. 15. From 0 to 35% emissions reduction, there are many low-cost renewable options that are currently actionable. Coal-fired electricity generation is not only the most carbon-

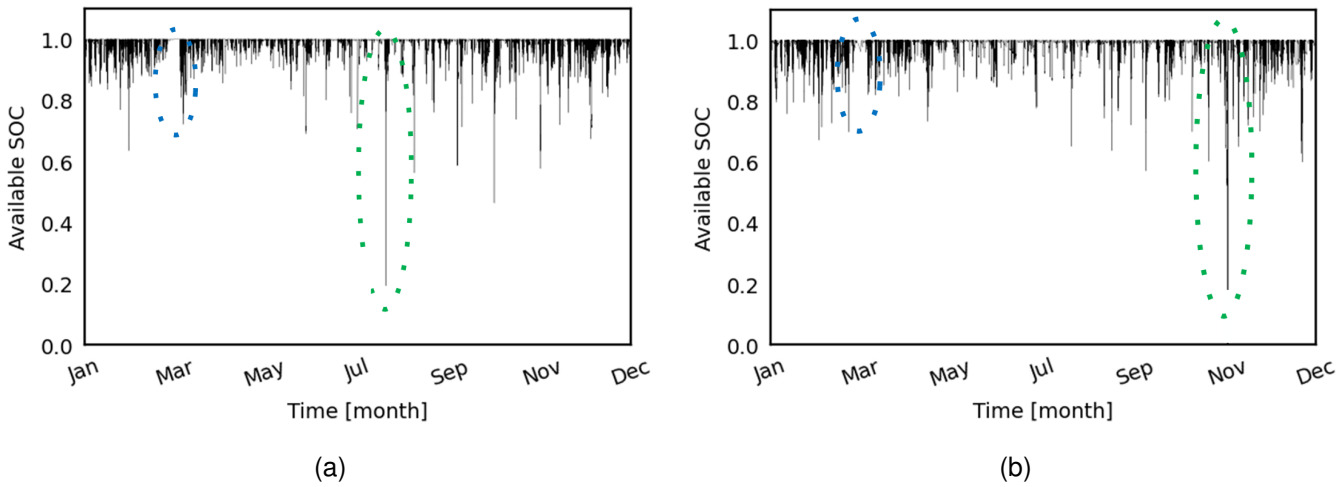

Fig. 14: Battery energy storage sized to solve minutely imbalances with plotted available SOC across the year for natural gas dominant generation with (a) 20GW of solar PV capacity, 10GW of wind capacity, rated power of 4.6GW and energy capacity of .41 GWh and (b) 6.5GW solar, 3.25GW wind, 2.5GW power, and .112GWh energy capacity. Dominant renewable generation significantly shifts the expected maximum peaking power to meet quick drops in VRE output and BESS energy capacity is nonlinearly related to renewable capacity.

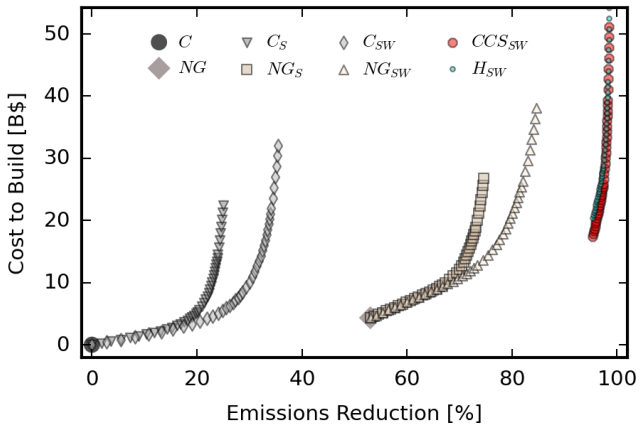

Fig. 15: CO2 emissions reduction vs. capital expenditure (CAPEX) cost to build relative to the current generation portfolio. Transition from coal dominant to NG dominant generation could reduce emissions by half. Solar and wind co-integration allows for increased VRE penetration as their generation timing is displaced from one another.

intensive generation technology, but also one of the least able to integrate intermittent renewables with diminishing returns for emissions reductions. For the existing portfolio, solar PV can be effectively integrated up to approximately 20% and furthermore, the combination of wind and solar allows for additional emissions reduction.

Transitioning from coal to natural gas generation results in a 50% reduction in emissions without renewable integration, as shown by the NG, the diamond, in Fig. 15. The reduction of CO2 emissions with increased renewable penetration stagnates without firm generation with faster ramping rates or shifting in time to meet unfulfilled demand, in line with expectations based on findings published by other authors, e.g. [22].

E. Levelized Cost of Energy per Generation Portfolio

A method is proposed to describe the Levelized Cost of Energy (LCOE) of generation portfolios consisting of multiple generation types. Additional LCOE was calculated starting from the current generation portfolio to compare the lifetime cost of electricity generation per subcase over a 30 year period. The LCOE per generation source was derived from methods published in the NREL's 2021 Annual Technology Baseline (ATB) [8] and adapted from the formulation described in [48] to summarize the portfolio cost by combining all generation technologies.

Combining LCOEs per generation type, the following relationship was used to approximate the combined LCOE ($/MWh) per portfolio:

$$LCOE = \frac{\sum_{i=1}^{7} FCR_i * CAPEX_i + FOM_i}{ED} * \frac{EG_i}{ED} + \sum_{i=1}^{7} (VOM_i + FC_i) * \frac{EG_i}{ED}, \tag{10}$$

where i is the generation type, including fossil-based and renewables; FCR the fixed charge rate or amount of revenue per dollar of investment collected annually to pay for the initial investment; FOM the annual fixed operation and maintenance cost; ED the total energy demand for the year of 2019; EG is the energy used from that generation type; VOM the variable operation and maintenance cost per MWh; and FC the fuel cost per MWh.

Technology-specific parameters, including *FCR, FOM, VOM, CAPEX,* and FC, were extracted from the NREL 2021 ATB based on 2019 data prior to Covid-19 related disruption. All fixed charge rates and operation and maintenance costs were assumed to follow conservative technology innovation with classes associated with the type of generation in Kentucky

TABLE III: Table of CAPEX construction cost and CO2 emissions rates per generation type

	Coal	NGCC	NG-CCS	NGCT	Hydrogen	Solar	Wind
CAPEX Cost to Build ($ per kW)	3,055	883	2,304	1,025	2,700	1,121	1,135
CO2 Emissions (lbs. per kWh)	2,000	800	80	1,200	80	N/A	N/A

specifically solar-utility PV class 7, land-based wind class 4, and hydropower NPD5 classifications. Hydrogen fuel is assumed to be readily available and equivalent to NGCC operation. The 30 year lifetime demand is directly copied from the sample year of minutely load. For each generation type, a ratio was implemented to LCOE per generation type to the total energy demand over the year, approximating LCOE if generation capacity was perfectly sized to annual utilization.

Trends in the cost and emissions resulting from renewable energy integration in the example study vary greatly depending on the dominant fossil fuel used for generation as shown in Fig. 16. The addition of solar PV and wind resources to coal-dominant generation results in an additional LCOE near zero as the cost of installing more renewable resources negates the operational costs of thermal generation up to a limit. After this limit, which is approximately 20% for solar PV and higher for solar and wind combined, increases to generation capacity require significant capital investment.

In the case study, natural gas and low carbon thermal generation dominant scenarios require significant capital investment for capacity development with an initial peak in LCOE. Higher renewable generation results in emission reduction and offsets operational costs and the need for some thermal generation capacity, resulting in a lower cost. As renewable generation increases, there is a limit for this trend, around 70% with solar and 80% with combined solar and wind.

Towards the development of low-carbon firm generation, carbon capture and sequestration, as well as green hydrogen generation and storage, are emerging technologies to maintain control of generation timing while greatly reducing emissions. Carbon capture and sequestration technologies (CCS) capture and restrict carbon emissions from generation plants, resulting in greatly reduced emissions for firm capability. Hydrogen energy storage and thermal generation is another alternative, allowing for green electrolysis or hydrogen fuel cell production using overgeneration and thermal generation when necessary to fill in the gapNew combustion turbine and combined cycle capacity may be further developed and integrated with hydrogen and carbon-capture to additionally reduce – or completely eliminate – carbon dioxide emissions.

F. Regional Case Study Specific Conclusions

The results of the case study indicate that moderate amounts of regionally dispersed solar PV generation, up to approximately 20%, could be integrated into the current portfolio at low costs without significant imbalances. Additional renewables up to 25% may be integrated without increases to additional LCOE if a balance of solar and wind generation is used due to their temporally shifted generation. At high renewable penetration, the benefit of additional renewable generation decreases as more generation has to be curtailed due to over-generation and the inability to shift generated energy to timely coordinate with load demand.

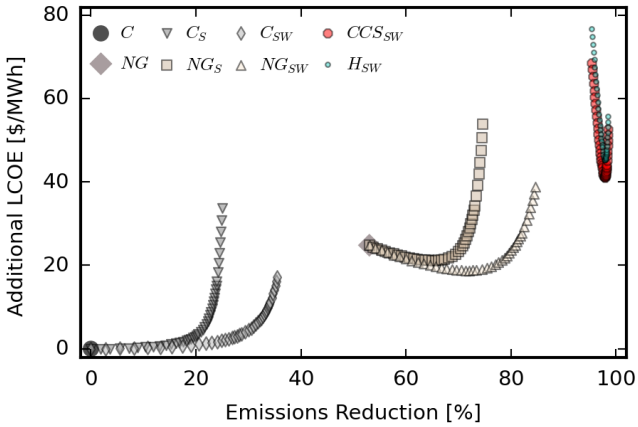

Fig. 16: Lifetime CO2 emissions reduction from current Kentucky generation vs. LCOE of generation portfolio construction and operation for a 30 year period. The introduction of VRE reduced emissions and the LCOE non-linearly increased with higher renewables penetration. Operation, maintenance, and fuel costs lead to an increased gap in cost between coal, natural gas, and low-carbon dominant cases.

Deep decarbonization and renewable integration, from 20 to 80%, can be achieved with the replacement of older coal-fired units, which are unable to effectively adjust output for variable generating resources, with new natural gas generation. Transitioning from coal to natural gas generation also results in a substantial reduction in emissions, with more than 50% reduction possible even without renewable integration. Furthermore, replacing coal with natural gas generation also enables the effective integration of double the renewable generation when comparing overgeneration because of increased operational flexibility. Firm generation is currently necessary to maintain system reliability, and the integration of resources with greater flexibility can allow more immediate and effective investment in renewable energy generation.

Complete decarbonization between 80 and 100% necessitates the implementation of higher cost, emerging technologies, such as large-scale energy storage, potentially from EVs in V2G operation, large-scale demand response and electric power distribution virtual power plants, advanced nuclear, carbon capture, or renewable green hydrogen sources. New natural gas combustion turbine and combined cycle capacity can be built using current state of the art technology and integrated with hydrogen and carbon-capture to further reduce — or completely eliminate — carbon dioxide emissions. Current R&D is focused on improving the performance and efficiency and lowering implementation costs for such technologies.

VI. Conclusion

The method proposed for optimized economic dispatch employs a minute-based approach that is able to consider the fast changes specific to variable renewable energy (VRE)

generation and required measures in order to ensure the balanced operation of the electric power system. The method has been implemented with differential evolution algorithms and demonstrated through year-long simulations with detailed minutely resolution data for weather, load, and operational constraints, resulting in large-scale computational problems that have been paralleled and solved on high – performance computing (HPC) systems.

The generally applicable procedures have been applied for a regional case study in Kentucky, USA with eight different scenarios with varying mixtures of firm and renewable generation capacity, which provided examples for evaluating feasibility, estimating the overgeneration and the effectiveness of VRE integration, cost to build and LCOE per portfolio, carbon emissions reductions, and for establishing trends. The simulation results show that electricity generation with faster ramping natural gas, rather than coal, power plants is advantageous in providing operational flexibility and supporting larger scale integration of renewables. The proposed minute-based methods are also suitable for sizing energy storage systems, which can further support the very large penetration of renewable energy generation.

ACKNOWLEDGMENT

The support of the Louisville Gas and Electric and Kentucky Utilities, part of the PPL Corporation family of companies, is gratefully acknowledged. The support received by Mr. Donovin D. Lewis through an NSF Graduate Research Fellowship (NSF) under Grant No. 1839289 and through a University of Kentucky Otis A. Singletary Fellowship, by Mr. Evan S. Jones through a Department of Education (DoEd) GAANN Fellowship, and by Miss Rosemary E. Alden through an NSF Graduate Research Fellowship (NSF) under Grant No. 1839289 and through University of Kentucky, the L. Stanley Pigman Chair in Power Endowment is also gratefully acknowledged. Any opinions, findings, conclusions, or recommendations expressed in this material are those of the authors alone and do not necessarily reflect the views of the LG&E and KU, PPL, NSF, or DoEd.

REFERENCES

[1] "Global energy-related CO2 emissions by sector – Charts – Data & Statistics," https://www.iea.org/data-and-statistics/charts/global-energy-related-co2-emissions-by-sector, 2022.

[2] A. Burdick, N. Schlag, A. Au, R. Go, Z. Ming, and A. Olson, "Lighting a reliable path to 100% clean electricity: Evolving resource adequacy practices for a decarbonizing grid," *IEEE Power and Energy Magazine*, vol. 20, no. 4, pp. 30–43, 2022.

[3] *, "Clean Air Markets Program Data (CAMPD)," EPA, https://campd.epa.gov, Tech. Rep., 2022.

[4] *, "United States Energy Information Administration (EIA) Monthly Electric Generator Inventory," EIA, https://www.eia.gov/electricity/data/eia860m/archive/xls/january_generator2022.xlsx, Tech. Rep., 2022.

[5] *, "PPL's 2021 Climate Assessment Report," Pennsylvania Power and Light, https://www.pplweb.com/wp-content/uploads/2022/01/PPL_Corp-2021-Climate-Assessment_2022-01-04.pdf, Tech. Rep., Jan. 2022.

[6] *, "EIA 860M and LG&E and KU 2021 Integrated Resources Plan," Louisville Gas and Electric and Kentucky Utilities, https://psc.ky.gov/pscecf/2021-00393/rick.lovekamp%40lge-ku.com/10192021013101/5-LGE_KU_2021_IRP_Volume_III.pdf, Tech. Rep., 2021.

[7] *, "Geospatial Data Science," https://www.nrel.gov/gis/index.html, 2021.

[8] "2021 ATB | NREL," https://atb.nrel.gov/, 2021.

[9] M. S. Javed, T. Ma, J. Jurasz, F. A. Canales, S. Lin, S. Ahmed, and Y. Zhang, "Economic analysis and optimization of a renewable energy based power supply system with different energy storages for a remote island," *Renewable Energy*, vol. 164, pp. 1376–1394, 2021.

[10] C. F. Heuberger, I. Staffell, N. Shah, and N. M. Dowell, "A systems approach to quantifying the value of power generation and energy storage technologies in future electricity networks," *Computers & Chemical Engineering*, vol. 107, pp. 247–256, 2017, in honor of Professor Rafiqul Gani.

[11] K. van der Wiel, L. Stoop, B. van Zuijlen, R. Blackport, M. van den Broek, and F. Selten, "Meteorological conditions leading to extreme low variable renewable energy production and extreme high energy shortfall," *Renewable and Sustainable Energy Reviews*, vol. 111, pp. 261–275, 2019.

[12] M. Lauby and R. Villafranca, "Method to Model and Calculate Capacity Contributions of Variable Generation for Resource Adequacy Planning," NERC, https://www.nerc.com/pa/RAPA/ra/Reliability%20Assessments%20DL/IVGTF1-2.pdf, Tech. Rep., Mar. 2011.

[13] B. Lunz, P. Stöcker, S. Eckstein, A. Nebel, S. Samadi, B. Erlach, M. Fischedick, P. Elsner, and D. U. Sauer, "Scenario-based comparative assessment of potential future electricity systems – a new methodological approach using germany in 2050 as an example," *Applied Energy*, vol. 171, pp. 555–580, 2016.

[14] B. van Zuijlen, W. Zappa, W. Turkenburg, G. van der Schrier, and M. van den Broek, "Cost-optimal reliable power generation in a deep decarbonisation future," *Applied Energy*, vol. 253, p. 113587, 2019.

[15] W. Zappa, M. Junginger, and M. van den Broek, "Is a 100% renewable european power system feasible by 2050?" *Applied Energy*, vol. 233-234, pp. 1027–1050, 2019.

[16] M. R. Shaner, S. J. Davis, N. S. Lewis, and K. Caldeira, "Geophysical constraints on the reliability of solar and wind power in the united states," *Energy Environ. Sci.*, vol. 11, pp. 914–925, 2018.

[17] A. Phadke, D. Wooley, N. Abhyankar, U. Paliwal, and B. Paulos, "2035 The Report," Goldman School of Public Policy: University of California Berkeley, http://www.2035report.com/wp-content/uploads/2020/06/2035-Report.pdf, Tech. Rep., Jun. 2020.

[18] E. Larson, C. Greig, J. Jenkins, E. Mayfield, A. Pascale, C. Zhang, J. Drossman, R. Williams, S. Pacala, R. Socolow, E. Baik, R. Birdsey, R. Duke, R. Jones, B. Haley, E. Leslie, K. Paustian, and A. Swan, "Net-Zero America: Potential pathways, infrastucture, and impacts," Princeton University, https://netzeroamerica.princeton.edu/, Tech. Rep., Oct. 2021.

[19] K. Gyanwali, R. Komiyama, and Y. Fujii, "Deep decarbonization of integrated power grid of eastern south asia considering hydrogen and ccs technology," *International Journal of Greenhouse Gas Control*, vol. 112, p. 103515, 2021.

[20] J. D. Jenkins, M. Luke, and S. Thernstrom, "Getting to zero carbon emissions in the electric power sector," *Joule*, vol. 2, no. 12, pp. 2498–2510, 2018.

[21] M. Borasio and S. Moret, "Deep decarbonisation of regional energy systems: A novel modelling approach and its application to the italian energy transition," *Renewable and Sustainable Energy Reviews*, vol. 153, p. 111730, 2022.

[22] P. Denholm, D. J. Arent, S. F. Baldwin, D. E. Bilello, G. L. Brinkman, J. M. Cochran, W. J. Cole, B. Frew, V. Gevorgian, J. Heeter, B.-M. S. Hodge, B. Kroposki, T. Mai, M. J. O'Malley, B. Palmintier, D. Steinberg, and Y. Zhang, "The challenges of achieving a 100% renewable electricity system in the united states," *Joule*, vol. 5, no. 6, pp. 1331–1352, 2021.

[23] O. M. Akeyo, A. Patrick, and D. M. Ionel, "Study of renewable energy penetration on a benchmark generation and transmission system," *Energies*, vol. 14, no. 1, 2021.

[24] T. Kumano, "A functional optimization based dynamic economic load dispatch considering ramping rate of thermal units output," in *2011 IEEE/PES Power Systems Conference and Exposition*, 2011, pp. 1–8.

[25] T. Luz and P. Moura, "100% renewable energy planning with complementarity and flexibility based on a multi-objective assessment," *Applied Energy*, vol. 255, 2019-12.

[26] L. Montero, A. Bello, and J. Reneses, "A review on the unit commitment problem: Approaches, techniques, and resolution methods," *Energies*, vol. 15, no. 4, 2022.

[27] N. A. Sepulveda, J. D. Jenkins, F. J. de Sisternes, and R. K. Lester, "The role of firm low-carbon electricity resources in deep decarbonization of power generation," *Joule*, vol. 2, no. 11, pp. 2403–2420, 2018.

[28] K. Guerra, P. Haro, R. Gutiérrez, and A. Gómez-Barea, "Facing the high share of variable renewable energy in the power system: Flexibility and stability requirements," *Applied Energy*, vol. 310, p. 118561, 2022.
[29] B. S. Palmintier and M. D. Webster, "Impact of operational flexibility on electricity generation planning with renewable and carbon targets," *IEEE Transactions on Sustainable Energy*, vol. 7, no. 2, pp. 672–684, 2016.
[30] J. Meus, K. Poncelet, and E. Delarue, "Applicability of a clustered unit commitment model in power system modeling," *IEEE Transactions on Power Systems*, vol. 33, no. 2, pp. 2195–2204, 2018.
[31] G. Morales-España and D. A. Tejada-Arango, "Modeling the hidden flexibility of clustered unit commitment," *IEEE Transactions on Power Systems*, vol. 34, no. 4, pp. 3294–3296, 2019.
[32] J. E. T. Bistline, "The importance of temporal resolution in modeling deep decarbonization of the electric power sector," *Environmental Research Letters*, vol. 16, no. 8, p. 084005, jul 2021.
[33] D. A. Tejada-Arango, G. Morales-España, S. Wogrin, and E. Centeno, "Power-based generation expansion planning for flexibility requirements," *IEEE Transactions on Power Systems*, vol. 35, no. 3, pp. 2012–2023, 2020.
[34] L. Bird and D. Lew, "Integrating wind and solar energy in the u.s. bulk power system: Lessons from regional integration studies," NREL, https://www.osti.gov/biblio/1051913, Tech. Rep., 9 2012.
[35] Y. Li, J. Wang, D. Zhao, G. Li, and C. Chen, "A two-stage approach for combined heat and power economic emission dispatch: Combining multi-objective optimization with integrated decision making," *Energy*, vol. 162, pp. 237–254, 2018.
[36] M. C. Peel, B. L. Finlayson, and T. A. McMahon, "Updated world map of the köppen-geiger climate classification," *Hydrology and Earth System Sciences*, vol. 11, no. 5, pp. 1633–1644, 2007.
[37] R. Storn and K. Price, "Differential Evolution - A Simple and Efficient Heuristic for Global Optimization over Continuous Spaces," *Journal of Global Optimization*, vol. 11, no. 4, pp. 341–359, 1997.
[38] "Kentucky Mesonet at WKU," http://www.kymesonet.org/, 2022.
[39] "E.W. Brown Solar Facility historical data | LG&E and KU," http://lge-ku.com/live-solar-generation/historical-data, 2022.
[40] *, "BAL-002-1," North American Electric Reliability Corporation, https://www.nerc.com/pa/Stand/Pages/BAL002-1RI.aspx, Tech. Rep., 2015.
[41] E. Ela and M. O'Malley, "Studying the variability and uncertainty impacts of variable generation at multiple timescales," *IEEE Transactions on Power Systems*, vol. 27, no. 3, pp. 1324–1333, 2012.
[42] S. Surender Reddy, P. R. Bijwe, and A. R. Abhyankar, "Real-time economic dispatch considering renewable power generation variability and uncertainty over scheduling period," *IEEE Systems Journal*, vol. 9, no. 4, pp. 1440–1451, 2015.
[43] *, "Life Cycle Greenhouse Gas Emissions from Electricity Generation: Update," NREL, https://www.nrel.gov/docs/fy21osti/80580.pdf, Tech. Rep., Sep. 2021.
[44] Y.-Y. Hong and G. F. D. Apolinario, "Uncertainty in unit commitment in power systems: A review of models, methods, and applications," *Energies*, vol. 14, no. 20, 2021.
[45] J. Kiviluoma, N. Helistö, N. Putkonen, C. Smith, M. Koivisto, M. Korpås, D. Flynn, L. Söder, E. Taibi, and A. Guminski, "Flexibility from the electrification of energy: How heating, transport, and industries can support a 100% sustainable energy system," *IEEE Power and Energy Magazine*, vol. 20, no. 4, pp. 55–65, 2022.
[46] H. Gong, R. E. Alden, and D. M. Ionel, "Stochastic battery soc model of ev community for v2g operations using cta-2045 standards," in *2022 IEEE Transportation Electrification Conference & Expo (ITEC)*, 2022, pp. 1144–1147.
[47] C. Crozier, C. Quarton, N. Mansor, D. Pagnano, and I. Llewellyn, "Modelling of the ability of a mixed renewable generation electricity system with storage to meet consumer demand," *Electricity*, vol. 3, no. 1, pp. 16–32, 2022.
[48] C. S. Lai and M. D. McCulloch, "Levelized cost of electricity for solar photovoltaic and electrical energy storage," *Applied Energy*, vol. 190, pp. 191–203, 2017.